

Cavity-loss induced plateau in coupled cavity QED array

Tatsuro Yuge,¹ Kenji Kamide,² Makoto Yamaguchi,¹ and Tetsuo Ogawa¹

¹*Department of Physics, Osaka University, Machikaneyama-Cho, Toyonaka, Osaka, 560-0043, Japan*

²*Institute of Industrial Science, the University of Tokyo, Komaba, Meguro-ku, Tokyo, 153-8505, Japan*
(Dated: February 27, 2022)

Nonequilibrium steady states are investigated in a coupled cavity QED array system which is pumped by a thermal bath and dissipated through cavity loss. In the coherent (non-zero photon amplitude) phase, plateau regions appear, where the steady states become unchanged against the variation of the chemical potential of the thermal bath. The cavity loss plays a crucial role for the plateaus: the plateaus appear only if the cavity loss exists, and the photon leakage current, which is induced by the loss, is essential to the mechanism of the plateaus.

PACS numbers: 42.50.Pq, 03.75.Kk

Introduction.—In recent years, much attention has been paid to coupled cavity QED arrays. In these systems, the effective photon-photon interaction in each cavity and photon hopping between cavities lead to rich quantum many-body phenomena of photons [1, 2]. For example, in equilibrium states, these systems exhibit quantum phase transitions between the “incoherent (or Mott insulator)” and “coherent (or superfluid)” phases [3–10]. Nonequilibrium states in these systems have been also investigated [11–19]. Most of the works have focused on the nonequilibrium effects of the pumping and dissipation on the properties observed in equilibrium states; e.g., signatures of the two phases in nonequilibrium states. However, phenomena genuinely characteristic to nonequilibrium states in the systems remain unexplored.

Apart from the coupled cavity QED array, examples of this kind of phenomena are seen in “nonequilibrium phase transitions,” such as the pattern formation outside equilibrium [20], dissipative structure [21], and lasing phenomena [22]. These are observed not in equilibrium states but only in nonequilibrium states. It is important to find such phenomena from the viewpoint that they can be used as test models for nonequilibrium statistical mechanics and thermodynamics.

In this paper, we report that another genuine nonequilibrium phenomenon can occur in a coupled cavity QED array that is pumped by a thermal bath and dissipated through cavity loss. We find that in the coherent phase there exist plateau regions where the states of the array system becomes unchanged to the variation of the chemical potential of the thermal bath. We show that the plateau emerges only if the cavity loss (dissipation) exists, which implies that the nonequilibrium effect is crucial for this phenomenon.

Setup.—We consider a cavity array that is connected to two baths. An illustration of the total system (array + baths) is shown in Fig. 1. Each cavity contains a two-level system (TLS) which is continuously excited through the coupling (excitation exchange) with the pumping bath (TLS bath). The pumping bath is in an equilibrium

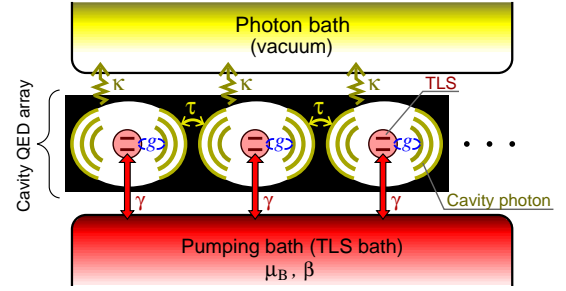


FIG. 1. (Color online) An illustration of the setup, consisting of a cavity QED array, a pumping bath (equilibrium state with the chemical potential μ_B and inverse temperature β), and a photon bath (vacuum state). Each cavity photon couples with a two-level system (TLS) (coupling constant g), with neighboring cavity photons (hopping constant τ), and with the photon bath (which induces the cavity loss κ). Each TLS is incoherently pumped (rate γ) by the pumping bath.

state characterized by the chemical potential μ_B and inverse temperature β . Thus the TLSs in the cavity array are incoherently pumped (rate γ). The photon mode in each cavity interacts with the TLS in the cavity (coupling constant g) and is coupled with the photons in the neighboring cavities through mode overlap (hopping constant τ). It is also coupled with the photon bath (vacuum), which induces the cavity loss κ .

The coupled cavity QED array is described by the Jaynes-Cummings-Hubbard Hamiltonian ($\hbar = 1$) [3]:

$$\hat{H}_S = \sum_i \hat{H}_i^{\text{JC}} - \tau \sum_{\langle ij \rangle} \hat{a}_i^\dagger \hat{a}_j, \quad (1)$$

$$\hat{H}_i^{\text{JC}} = \omega_0 \hat{\sigma}_i^+ \hat{\sigma}_i^- + \omega_0 \hat{a}_i^\dagger \hat{a}_i + g(\hat{\sigma}_i^+ \hat{a}_i + \hat{\sigma}_i^- \hat{a}_i^\dagger), \quad (2)$$

where i and j represent the site indices of the cavities, $\hat{\sigma}_i^+$ and $\hat{\sigma}_i^-$ are the raising and lowering operators of the TLS, and \hat{a}_i^\dagger and \hat{a}_i are the creation and annihilation operators of the cavity photon in the i th cavity. The first term in Eq. (1) is the Jaynes-Cummings Hamiltonian for single cavities given by Eq. (2), and the second term is

the hopping of the photons between the neighboring cavities ($\langle ij \rangle$ means the nearest neighbor sites). We assume that the transition frequency of the TLS and the cavity frequency are resonant and the same for all of the cavities (denoted by ω_0).

To obtain insight over the steady-state properties of the pumped-dissipative system, we employ a mean-field (MF) approximation and quantum master equation (QME). We introduce the steady-state average photon field $\psi(t) \equiv \langle \hat{a}_i \rangle_{ss}$ as the mean field. We assume that it oscillates with a single frequency μ in the rest frame: $\psi(t) = \psi e^{-i\mu t}$, where the amplitude ψ is a real number. After using the MF approximation [3] and transforming into the rotating frame with μ , we take the trace over the baths and use the Born-Markov approximation. Then we have the QME in the Schrödinger picture (within the rotating frame) [23]: $d\tilde{\rho}/dt = \mathcal{L}\tilde{\rho}$, where $\tilde{\rho}$ is the density matrix of the array system in the rotating frame. The QME superoperator \mathcal{L} is given by $\mathcal{L} = -i[\tilde{K}_S, \cdot] + \mathcal{L}_{\text{TLS}} + \mathcal{L}_{\text{ph}}$, where \tilde{K}_S is the effective system Hamiltonian in the rotating frame, and \mathcal{L}_{TLS} and \mathcal{L}_{ph} are the superoperators associated with the TLS and photon baths, respectively. We will describe the details in the last part of this paper. We determine the steady-state solution $\tilde{\rho}_{ss}(\psi, \mu)$ in the rotating frame by

$$\mathcal{L}\tilde{\rho}_{ss}(\psi, \mu) = 0. \quad (3)$$

Note that the solution $\tilde{\rho}_{ss}$ depends on ψ and μ . Then we have the self-consistent equation for the mean field:

$$\psi = \text{Tr}_S[\tilde{\rho}_{ss}(\psi, \mu)\hat{a}]. \quad (4)$$

By solving Eqs. (3) and (4) numerically, we determine the values of ψ and μ , and obtain the steady-state density matrix $\tilde{\rho}_{ss}$ of the MF-QME for the pumped-dissipative cavity QED array system. For the numerical calculation we set the cutoff for the maximum photon number in the cavity to 10.

Phase diagram.—First we investigate a phase diagram of the nonequilibrium steady states in the array system by employing ψ as the order parameter. Figure 2 depicts the regions for $\psi = 0$ and $\psi \neq 0$ as a function of the hopping constant τ and the chemical potential μ_B of the TLS bath. We refer to the region with $\psi = 0$ as incoherent phase and to the region with $\psi \neq 0$ as coherent phase. For comparison, we also show the phase boundary in the equilibrium states ($\kappa = 0$) by the dotted curve.

In small μ_B (weak pumping) regime, the phase boundary is almost the same as that of the equilibrium states. This implies that the array system is nearly equilibrium in this regime.

In larger μ_B (strong pumping) regime, by contrast, the coherent phase region shrinks compared with the equilibrium case. This results from a nonequilibrium effect; in this regime, the number of the cavity photons increases, so that the effect of the cavity loss becomes larger. Since

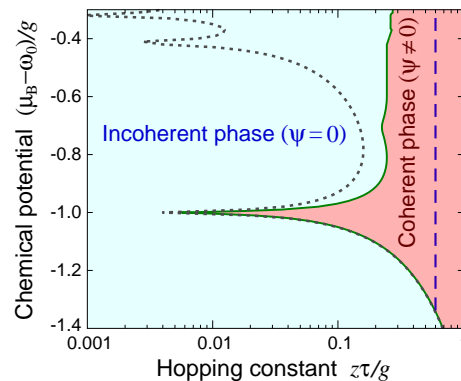


FIG. 2. (Color online) Steady-state phase diagram of the pumped-dissipative cavity QED array system. The vertical and horizontal axes are respectively the chemical potential μ_B of the TLS bath and the hopping constant τ (z is the number of the nearest neighbor sites). The boundary between the incoherent ($\psi = 0$) and coherent ($\psi \neq 0$) phases is plotted. The parameter values are: $1/\beta g = 0.001$, $\gamma/g = 0.02$, and $\kappa/g = 0.007$. The dotted curve is the phase boundary for the equilibrium case ($\kappa = 0$). The dashed line ($z\tau/g = 0.6$) is the one along which the results in Fig. 3 are plotted.

the loss destroys the coherence of the system, the area of the coherent phase decreases in this regime.

Main result.—In Fig. 3(a), we plot μ_B -dependence of the frequency μ and the average photon number per cavity $\langle N_{\text{ph}} \rangle_{ss} \equiv \text{Tr}_S[\tilde{\rho}_{ss}\hat{a}^\dagger\hat{a}]$ in the coherent phase along the dashed line in Fig. 2 [24]. In small μ_B (weak pumping) regime, we observe $\mu \simeq \mu_B$. We note that in the equilibrium states $\mu = \mu_B$ holds. Therefore this result is consistent with the fact that the array system is near to equilibrium in this regime.

In larger μ_B regime, we observe plateaus both in μ and $\langle N_{\text{ph}} \rangle_{ss}$; i.e., there are regions of μ_B where μ and $\langle N_{\text{ph}} \rangle_{ss}$ take constant values. We numerically confirm that the steady-state density matrix $\tilde{\rho}_{ss}$ itself is unchanged in the plateau regions. We note that the cavity loss is crucial for the emergence of the plateaus because $\mu = \mu_B$ holds for $\kappa = 0$ (in the equilibrium states). Furthermore, in the supplement [25], we will show that the chemical potential at the beginning of the first plateau [pointed with the up arrow in Fig. 3(a)] increases as κ decreases and that it enters the unstable region [8] in the limit of $\kappa \rightarrow 0$. These cavity-loss induced plateaus, which are our main findings in this paper, seem counterintuitive since the loss usually smears out (rather than generates) sharp-cut phenomena. We also note that the incoherent pumping is necessary to observe the plateaus because we see them in the dependence on μ_B . The emergence of the plateaus implies that the properties of the cavity QED array system are completely stable to the uncertainty of μ_B ; for example, photoluminescence spectrum and photon statistics as well as μ and $\langle N_{\text{ph}} \rangle_{ss}$ are unchanged with the variation of μ_B .

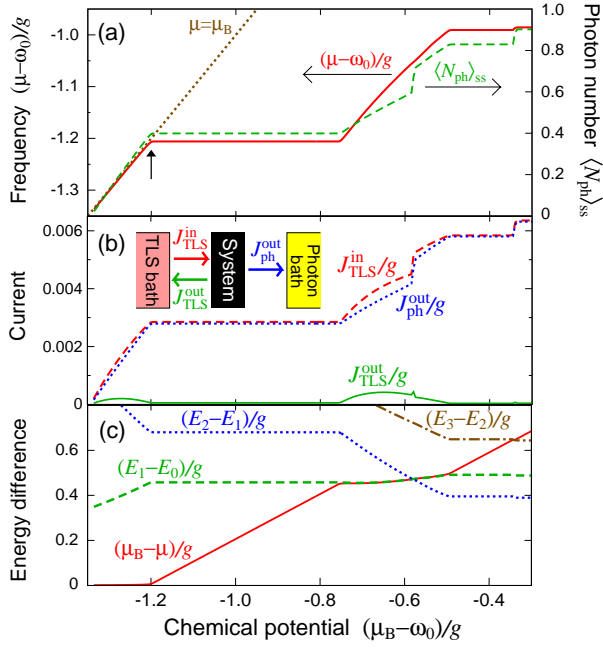


FIG. 3. (Color online) (a) Photon frequency μ (solid line; left vertical axis) and photon number $\langle N_{ph} \rangle_{ss}$ (dashed line; right vertical axis) as functions of the TLS bath chemical potential μ_B , which are calculated along the dashed line ($z\tau/g = 0.6$) in Fig. 2. The dotted line represents $\mu = \mu_B$. (b) Currents between the system and baths. The solid, dashed, and dotted lines represent J_{TLS}^{out} (from the system to TLS bath), J_{TLS}^{in} (from the TLS bath to system), and J_{ph}^{out} (from the system to photon bath), respectively. The inset shows an illustration of the currents. (c) $\mu_B - \mu$ (solid line), $E_1 - E_0$ (dashed line), $E_2 - E_1$ (dotted line), and $E_3 - E_2$ (dash-dotted line) plotted against μ_B , where E_q ($q = 0, 1, 2, 3$) are the eigenenergies of \tilde{K}_S . The parameter values are the same as those in Fig. 2.

within the plateaus.

Mechanism.—We here discuss the mechanism of the plateaus. For this purpose, we investigate the relationship of the plateaus with the currents and energy differences.

As we mentioned, the plateaus are induced by the cavity loss. This leads us to expect that quantities directly related to the cavity loss are essential to the mechanism. A typical one is the photon current that leaks to the photon bath. Therefore we first investigate the relationship with the currents.

In Fig. 3(b), we plot the currents: $J_{TLS}^{out} \equiv -\text{Tr}_S[\hat{\sigma}^+ \hat{\sigma}^- \mathcal{L}_{TLS}^- \tilde{\rho}_{ss}]$ (from the system to TLS bath), $J_{TLS}^{in} \equiv \text{Tr}_S[\hat{\sigma}^+ \hat{\sigma}^- \mathcal{L}_{TLS}^+ \tilde{\rho}_{ss}]$ (from the TLS bath to system), and $J_{ph}^{out} \equiv -\text{Tr}_S[\hat{a}^\dagger \hat{a} \mathcal{L}_{ph} \tilde{\rho}_{ss}]$ (from the system to photon bath) [26], where the superoperators \mathcal{L}_{TLS}^\pm and \mathcal{L}_{ph} are respectively given by Eqs. (6) and (5) (see the last part). A schematic illustration of the currents are shown in the inset of Fig. 3(b). We observe that $J_{TLS}^{in} \simeq J_{ph}^{out}$ and $J_{TLS}^{out} \simeq 0$ in the plateaus (note that

$J_{TLS}^{in} = J_{TLS}^{out} + J_{ph}^{out}$ holds in the steady states).

Next we investigate the relationship with the energy differences. As we mentioned, the plateaus are observed in the dependence on the chemical potential μ_B . In the QME, especially in the superoperator \mathcal{L}_{TLS} , $\mu_B - \mu$ (rather than μ_B itself) and the eigenenergy differences appear [see the below of Eq. (6)]. Therefore we investigate $\mu_B - \mu$ and the eigenenergy differences.

In Fig. 3(c), we plot $\mu_B - \mu$ and $E_q - E_{q-1}$, where E_q ($q = 0, 1, 2, 3$) are the eigenenergies for the ground and q th excited states of the effective Hamiltonian \tilde{K}_S . We observe that $E_1 - E_0$ and $E_3 - E_2$ cross with $\mu_B - \mu$ respectively at the ends of the first and second plateaus, whereas $E_2 - E_1$ crosses with $\mu_B - \mu$ in the transition region between the first and second plateaus.

From these observations, we have a following mechanism scenario of the plateaus. First we discuss the first plateau. When $\mu_B - \mu < E_1 - E_0$, i.e., before the end of the first plateau, the ground state is the only channel available for pumping from the TLS bath. Before the first plateau starts, J_{TLS}^{in} is a convex function of μ_B , whereas J_{ph}^{out} is almost proportional to μ_B . These behaviors of the currents possibly result from the fact that, for each single pumping channel, $\hat{\sigma}^+ \hat{\sigma}^-$ is bounded above whereas $\hat{a}^\dagger \hat{a}$ is not. Due to these behaviors, J_{ph}^{out} can catch up with J_{TLS}^{in} at certain μ_B . However, it can not go over J_{TLS}^{in} since $J_{ph}^{out} \leq J_{TLS}^{in}$ holds in the steady states. Therefore the first plateau starts from this value of μ_B . As μ_B increases further, $\mu_B - \mu$ gets equal to $E_1 - E_0$, which results in the open of a new channel – the first excited state – for pumping from the TLS bath. Therefore the system can go out of the first plateau when $\mu_B - \mu \simeq E_1 - E_0$. This scenario requires the existence of J_{ph}^{out} , which is consistent with the fact that the cavity loss is crucial for the plateaus.

Similarly, the beginning of the second plateau is the point where J_{ph}^{out} catches up with J_{TLS}^{in} again. In this case, we should note that $\mu_B - \mu$ crosses with $E_2 - E_1$ before the second plateau starts. Thus we do not observe the end of the plateau at this point although the pumping channel of the second excited state opens. Instead, we observe the effect of this channel open as the jumps in $\langle N_{ph} \rangle_{ss}$ [Fig. 3(a)] and in the currents [Fig. 3(b)]. The end of the second plateau is the point where $\mu_B - \mu$ crosses with $E_3 - E_2$ and the pumping channel of the third excited state opens.

Finally we remark that in the plateau regions the input excitation of the TLSs is almost perfectly converted to the output of the photons because $J_{TLS}^{in} \simeq J_{ph}^{out}$ holds there. In this sense, conversion efficiency of this system in the plateaus is nearly 100%.

Details of the MF-QME.—The Hamiltonian of the total system (array + baths) is given by $\hat{H}_{tot} = \hat{H}_S + \hat{H}_{bath}^{TLS} + \hat{H}_{bath}^{ph}$, where \hat{H}_S is given by Eq. (1), and \hat{H}_{bath}^{TLS} and \hat{H}_{bath}^{ph} are respectively the Hamiltonians of the TLS

and photon baths including the system-bath interactions. We assume that the baths are sufficiently larger than the array system, so that the TLS bath remains in the equilibrium state with μ_B and β and the photon bath remains in the vacuum. We obtain the MF-QME for the array system as follows.

First, we explain the MF approximation. As we mentioned before, we introduce the oscillating photon field as the mean field: $\psi(t) \equiv \langle \hat{a}_i \rangle_{ss} = \psi e^{-i\mu t}$. Then we use the MF approximation [3]: $\hat{a}_i^\dagger \hat{a}_j \simeq \psi e^{i\mu t} \hat{a}_j + \psi e^{-i\mu t} \hat{a}_i^\dagger - \psi^2$. Substituting this into the second term in Eq. (1), we obtain the MF system Hamiltonian as a sum over the single sites. We can thus reduce the problem to the single-site one, and will omit the site index: $\hat{H}_S^{\text{MF}} = \hat{H}^{\text{JC}} - z\tau(\psi e^{i\mu t} \hat{a} + \psi e^{-i\mu t} \hat{a}^\dagger - \psi^2)$, where z is the number of the nearest neighbor sites. Furthermore, by transforming into the rotating frame with the frequency μ , we eliminate the time dependence in \hat{H}_S^{MF} ; i.e., $\tilde{H}_S^{\text{MF}} = e^{i\mu \hat{N}_{\text{tot}} t} \hat{H}_S^{\text{MF}} e^{-i\mu \hat{N}_{\text{tot}} t} = \hat{H}^{\text{JC}} - z\tau(\psi \hat{a} + \psi \hat{a}^\dagger - \psi^2)$, where $\hat{N}_{\text{tot}} = \hat{N}_S + \hat{N}_{\text{bath}}$, $\hat{N}_S = \hat{a}^\dagger \hat{a} + \hat{\sigma}^+ \hat{\sigma}^-$ is the total number of photon and TLS excitations in the cavity, and \hat{N}_{bath} is the excitation number in the baths. Then we have the von Neumann equation for the density matrix $\tilde{\rho}_{\text{tot}}$ of the total system in the rotating frame as $d\tilde{\rho}_{\text{tot}}(t)/dt = -i[\tilde{H}_S^{\text{MF}} + \hat{H}_{\text{bath}}^{\text{TLS}} + \hat{H}_{\text{bath}}^{\text{ph}} - \mu \hat{N}_{\text{tot}}, \tilde{\rho}_{\text{tot}}(t)]$.

Next, we explain the QME. Starting from the above von Neumann equation, we take the trace over the baths and use the Born-Markov approximation to obtain the QME in the Schrödinger picture (within the rotating frame) [23]: $d\tilde{\rho}/dt = \mathcal{L}\tilde{\rho}$, where $\tilde{\rho} = \text{Tr}_{\text{bath}} \tilde{\rho}_{\text{tot}}$ and $\mathcal{L} = -i[\tilde{K}_S, \cdot] + \mathcal{L}_{\text{ph}} + \mathcal{L}_{\text{TLS}}$. Here $\tilde{K}_S = \tilde{H}_S^{\text{MF}} - \mu \hat{N}_S$ is the effective system Hamiltonian in the rotating frame. The superoperator \mathcal{L}_{ph} associated with the photon bath is given by

$$\mathcal{L}_{\text{ph}} \tilde{\rho} = -\frac{\kappa}{2} (\hat{a}^\dagger \hat{a} \tilde{\rho} + \tilde{\rho} \hat{a}^\dagger \hat{a} - 2\hat{a} \tilde{\rho} \hat{a}^\dagger), \quad (5)$$

where κ is the cavity loss rate. To rewrite the superoperator \mathcal{L}_{TLS} associated with the TLS bath into a tractable form, we introduce eigenoperators of \tilde{K}_S as follows. We denote by $\hat{P}(E_q)$ the projection operator onto the eigenspace belonging to E_q (eigenvalue of \tilde{K}_S). Then we define eigenoperators: $\hat{\sigma}_\omega^\pm = \sum_q \hat{P}(E_q \pm \omega) \hat{\sigma}^\pm \hat{P}(E_q)$. By using these operators we can write \mathcal{L}_{TLS} as $\mathcal{L}_{\text{TLS}} = \mathcal{L}_{\text{TLS}}^+ + \mathcal{L}_{\text{TLS}}^-$ [23], where

$$\begin{aligned} \mathcal{L}_{\text{TLS}}^\pm \tilde{\rho} &= -\frac{\gamma}{2} \sum_\omega f^\pm(\omega) \left[\hat{\sigma}^\mp \hat{\sigma}_\omega^\pm \tilde{\rho} + \tilde{\rho} \hat{\sigma}_\omega^\mp \hat{\sigma}^\pm - \hat{\sigma}^\pm \tilde{\rho} \hat{\sigma}_\omega^\mp - \hat{\sigma}_\omega^\pm \tilde{\rho} \hat{\sigma}^\mp \right]. \end{aligned} \quad (6)$$

Here γ is the pumping rate, the ω -sum is over the eigenvalue differences, $f^+(\omega) = 1/\{1 + \exp \beta[\omega - (\mu_B - \mu)]\}$ is the Fermi distribution function, and $f^-(\omega) = 1 - f^+(\omega)$. Note that, if the cavity loss is absent ($\kappa = 0$), \mathcal{L}_{TLS} leads the array system to the equilibrium state with the chemical potential μ_B and inverse temperature β .

Conclusion.—We have investigated the nonequilibrium steady states in a coupled cavity QED array system that is incoherently pumped by a thermal bath for the TLS and dissipated by the vacuum of the photon. We have determined a steady-state phase diagram by employing the photon amplitude ψ as the order parameter. In the coherent phase (region with $\psi \neq 0$), we have found that there exist cavity-loss induced plateaus where the state of the array system becomes unchanged as a function of the chemical potential μ_B of the TLS bath. We have proposed a mechanism of the plateaus. There are two essential elements in the proposed mechanism: one is the existence of discrete energy levels (or energy gap) in the system, and the other is that the output current to one of the baths can catch up with the input current from the other bath (the bounded excitation number of the TLS and unbounded photon number would be the origin in our case). Therefore, if our scenario is correct, similar plateau phenomena should be observed in other systems which have these elements.

This work was supported by a JSPS Research Fellowship for Young Scientists (No. 24-1112) and by the JSPS through the FIRST Program. K. K. is also supported by the Project for Developing Innovation Systems of MEXT.

-
- [1] M. J. Hartmann, F. G. S. L. Brandão, and M. B. Plenio, *Laser Photonics Reviews*, **2**, 527 (2008).
 - [2] A. Tomadin and R. Fazio, *J. Opt. Soc. Am. B* **27**, A130 (2010).
 - [3] A. D. Greentree, C. Tahan, J. H. Cole, and L. C. L. Hollenberg, *Nat. Phys.* **2**, 856 (2006).
 - [4] M. J. Hartmann, F. G. S. L. Brandão, and M. B. Plenio, *Nat. Phys.* **2**, 849 (2006).
 - [5] D. G. Angelakis, M. F. Santos, and S. Bose, *Phys. Rev. A* **76**, 031805 (2007).
 - [6] D. Rossini and R. Fazio, *Phys. Rev. Lett.* **99**, 186401 (2007).
 - [7] M. I. Makin, J. H. Cole, C. Tahan, L. C. L. Hollenberg, and A. D. Greentree, *Phys. Rev. A* **77**, 053819 (2008).
 - [8] J. Koch and K. Le Hur, *Phys. Rev. A* **80**, 023811 (2009).
 - [9] M. Schiró, M. Bordyuh, B. Öztóp, and H. E. Türeci, *Phys. Rev. Lett.* **109**, 053601 (2012).
 - [10] K. Kamide, M. Yamaguchi, T. Kimura, and T. Ogawa, *Phys. Rev. A* **87**, 053842 (2013).
 - [11] I. Carusotto, D. Gerace, H. E. Türeci, S. De Liberato, C. Ciuti, and A. Imamoglu, *Phys. Rev. Lett.* **103**, 033601 (2009).
 - [12] M. J. Hartmann, *Phys. Rev. Lett.* **104**, 113601 (2010).
 - [13] A. Tomadin, V. Giovannetti, R. Fazio, D. Gerace, I. Carusotto, H. E. Türeci, and A. Imamoglu, *Phys. Rev. A* **81**, 061801(R) (2010).
 - [14] S. Ferretti, L. C. Andreani, H. E. Türeci, and D. Gerace, *Phys. Rev. A* **82**, 013841 (2010).
 - [15] S. Schmidt, D. Gerace, A. A. Houck, G. Blatter, and H. E. Türeci, *Phys. Rev. B* **82**, 100507(R) (2010).
 - [16] M. Knap, E. Arrigoni, W. von der Linden, and J. H. Cole, *Phys. Rev. A* **83**, 023821 (2011).

- [17] F. Nissen, S. Schmidt, M. Biondi, G. Blatter, H. E. Türeci, and J. Keeling, Phys. Rev. Lett. **108**, 233603 (2012).
- [18] T. Grujic, S. R. Clark, D. Jaksch, and D. G. Angelakis, New J. Phys. **14**, 103025 (2012).
- [19] J. Jin, D. Rossini, R. Fazio, M. Leib, and M. J. Hartmann, Phys. Rev. Lett. **110**, 163605 (2013).
- [20] M. C. Cross and P. C. Hohenberg, Rev. Mod. Phys. **65**, 851 (1993).
- [21] G. Nicolis, and I. Prigogine, *Self-organization in Nonequilibrium Systems, from Dissipative Structures to Order through Fluctuations* (Wiley, New York, 1977).
- [22] H. Haken, *Light, volume 2: Laser light dynamics* (Elsevier North-Holland, New York, 1985).
- [23] H. P. Breuer and F. Petruccione, *The Theory of Open Quantum Systems* (Oxford University Press, London, 2002).
- [24] In the incoherent phase, the photon frequency μ is indefinite because the photon amplitude ψ vanishes.
- [25] See Supplemental Material.
- [26] There is no current from the photon bath to system because the photon bath is in the vacuum state.

**SUPPLEMENTAL MATERIAL FOR
“CAVITY-LOSS INDUCED PLATEAU IN
COUPLED CAVITY QED ARRAY”**

Cavity-loss dependence of the beginning of the first plateau

Here we investigate the dependence of the first plateau on the cavity loss κ to obtain data that support the essentiality of the cavity loss for the plateaus. We denote the chemical potential at the beginning of the first plateau by μ_B^{1st} , which is pointed with the up arrow in Fig. 3(a).

We plot μ_B^{1st} (circle symbols) as a function of κ in Fig. A. We observe that μ_B^{1st} increases as κ becomes smaller. This is consistent with the essentiality of the cavity loss for the plateaus.

We also evaluate μ_B^{1st} from the equilibrium state as follows. As we mentioned in the main text, we can identify μ_B^{1st} with the point where J_{ph}^{out} becomes equal to J_{TLS}^{in} . Since the system is near to an equilibrium state for $\mu_B < \mu_B^{1st}$, we expect that we can calculate J_{ph}^{out} and J_{TLS}^{in} for $\mu_B < \mu_B^{1st}$ in good approximation by using the equilibrium state. We thus evaluate μ_B^{1st} from the approximate J_{ph}^{out} and J_{TLS}^{in} . For the practical calculation, we use the ground state $|E_0\rangle$ as the equilibrium state because the temperature of the TLS bath ($1/\beta g = 0.001$) is sufficiently lower than the eigenenergy difference $[(E_1 - E_0)/g > 0.3]$; see Fig. 3(c)]. In this case we have $J_{ph}^{out} = \kappa \langle E_0 | \hat{a}^\dagger \hat{a} | E_0 \rangle$ and $J_{TLS}^{in} = \gamma |\langle E_0 | \hat{\sigma}^- | E_0 \rangle|^2$. We note that we set $\mu_B - \mu$ to $+0$ to obtain the latter. In Fig. A, we plot μ_B (triangle symbols) where the thus-evaluated J_{ph}^{out} and J_{TLS}^{in} get equal. We see that the result provides a good approximation to μ_B^{1st} . We also observe that the approximate μ_B^{1st} approaches to a finite value as κ decreases.

To see this more clearly, we use another evaluation of μ_B^{1st} in the following analysis. First we note that when we approximate the steady state by the ground state we have $J_{ph}^{out} = \kappa \langle \hat{a}^\dagger \hat{a} \rangle$ and $J_{TLS}^{in} = \gamma |\langle \hat{\sigma}^- \rangle|^2$. Next, from the steady-state equation for $\langle \hat{a} \rangle$, we have a relationship $\langle \hat{\sigma}^- \rangle = -(\omega_0 - \mu - z\tau - i\kappa/2) \langle \hat{a} \rangle / g$. Substituting this relationship into J_{TLS}^{in} and equating J_{TLS}^{in} with J_{ph}^{out} (with $\mu = \mu_B^{1st}$), we have $|\omega_0 - \mu_B^{1st} - z\tau - i\kappa/2|^2 = \kappa \langle \hat{a}^\dagger \hat{a} \rangle / \gamma |\langle \hat{a} \rangle|^2$. Now we neglect $O(\kappa^2)$ term (since we consider small κ)

and approximate $\langle \hat{a}^\dagger \hat{a} \rangle \simeq |\langle \hat{a} \rangle|^2$ (since we consider the coherent phase). Then we obtain

$$(\mu_B^{1st} - \omega_0)/g = -z\tau/g - \sqrt{\kappa/\gamma}. \quad (A.1)$$

We plot this equation as the solid curve in Fig. A. We observe that this equation provides a good approximation to μ_B^{1st} . Equation (A.1) means that $(\mu_B^{1st} - \omega_0)/g$ converges to $-z\tau/g$ in the limit of $\kappa \rightarrow 0$. At first glance this may look inconsistent with the essentiality of the cavity loss for the plateaus. However, in the equilibrium case, the region with $(\mu_B - \omega_0)/g \geq -z\tau/g$ is unstable [1]. Therefore we conclude that the plateaus do not appear in the equilibrium situation ($\kappa = 0$). We thus show that the results in this supplement support the essentiality.

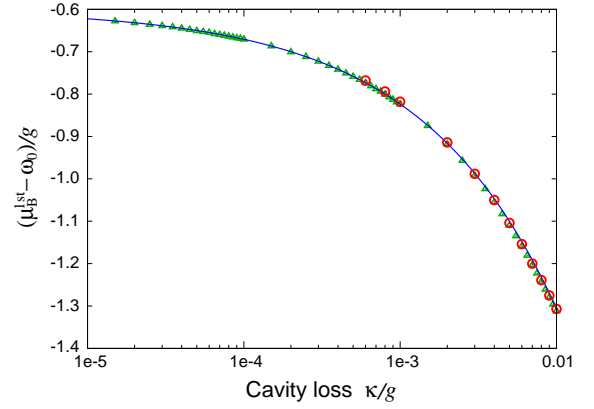


FIG. A. Chemical potential μ_B^{1st} at the beginning of the first plateau (circle symbols) as a function of the cavity loss κ . The cutoff for the maximum photon number in the cavity is set to 15 for $\kappa/g \geq 0.002$, 25 for $\kappa/g = 0.001, 0.0008$, and 30 for $\kappa/g = 0.0006$. Evaluation from the equilibrium state (with the cutoff photon number being 500) is plotted with the triangle symbols. The solid line is a plot of Eq. (A.1). The hopping constant $z\tau/g$ is set to 0.6. The other parameter values are the same as those in Fig. 2.

[1] J. Koch and K. Le Hur, Phys. Rev. A **80**, 023811 (2009).